

EXTENDED SCALAR SECTORS AT CURRENT AND FUTURE COLLIDERS

T. ROBENS

Ruder Boskovic Institute, Bijenicka cesta 54, 10000 Zagreb, Croatia

We here give a brief overview on the current status of selected models that extend the scalar sector of the Standard Model with additional matter states. We comment on current bounds as well as possible discovery prospects at current and future colliders.

1 Introduction

After the discovery of a particle that complies with the properties of the Higgs boson predicted by the Standard Model, particle physics has entered an exciting era. One important question is whether the scalar sector realized by Nature indeed corresponds to the one predicted by the SM, or whether the resonance at 125 GeV is a manifestation of a more extended scalar sector, and additional scalar states could be observed at current or future collider facilities.

2 Theoretical and experimental constraints

In general, the introduction of non SM-like terms in the potential can lead to massive mass-eigenstates and, successively, induce additional collider signatures. These predictions need to be confronted with constraints from both theoretical and experimental sources. We here list them for brevity and refer the reader to the corresponding references for more detail.

2.1 Theory constraints

Theoretical constraints include checks that the potential is bounded from below, perturbative unitarity, typically via requirements on the maximal eigenvalue for the $2 \rightarrow 2$ scalar scattering matrix using partial wave expansion, and perturbativity of the couplings. Tools which can be used for these checks include, among others, 2HDMC^{1,2} and ScannerS^{3,4}.

2.2 Experimental constraints

From the experimental side, one of the most important features that need to be met is the availability of a scalar particle that complies with the SM Higgs boson, including all current measurements (mass and signal strength). Furthermore, one needs to ensure agreement with electroweak precision measurements, null-searches at past and current colliders, and, for particles providing a dark matter candidate, agreement with astrophysical measurements such as relic density and direct detection bounds. Tools which enable comparison with collider results are e.g. HiggsBounds^{5,6,7,8,9,10,11} and HiggsSignals^{12,13,14,10,15}, while dark matter predictions can be obtained using MicrOMEGAs^{16,17}. These are confronted with experimental findings, i.e. latest results from the GFitter collaboration^{18,19,20} as well as astrophysical observables from the Planck collaboration²¹ and XENON1T²².

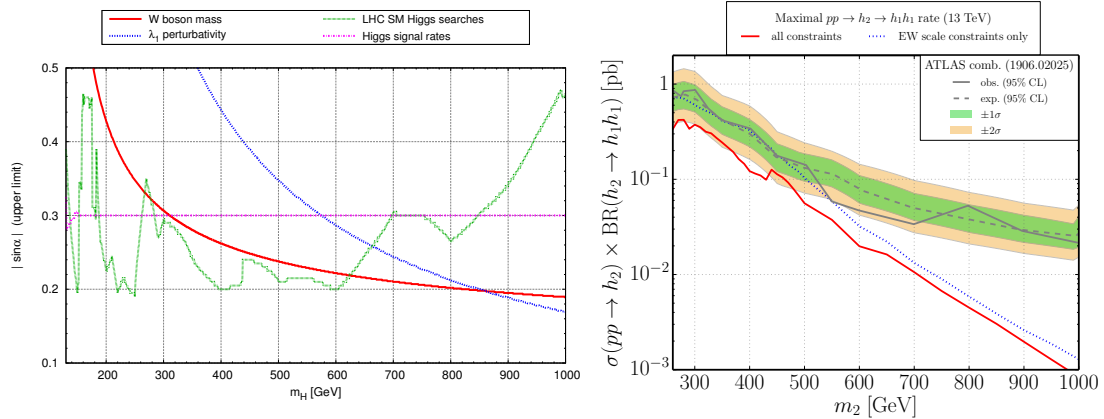


Figure 1 – Novel results for the singlet extension. *Left*: comparison of current constraints for a fixed value of $\tan\beta = 0.1$. *Right*: maximal $H \rightarrow hh$ allowed, with electroweak constraints at the electroweak scale (blue) or including RGE running to a higher scale (red), in comparison with results from the ATLAS combination.

3 Real singlet extension: novel results

We here discuss the \mathbb{Z}_2 symmetric real singlet extension of the SM, where we follow previous work on this model^{23,24,25,26,27,28}. We discuss the case where the \mathbb{Z}_2 symmetry is softly broken by a vacuum expectation value (vev) of the singlet field, inducing mixing between the gauge-eigenstates which introduces a mixing angle α . The model has in total 5 free parameters, out of which 2 are fixed by the measurement of the 125 GeV resonance mass and electroweak precision observables. This leaves

$$\sin\alpha, m_2, \tan\beta \equiv \frac{v}{v_s} \quad (1)$$

as free parameters of the model, where v (v_s) corresponds to the vev of the SM-like doublet (singlet) field. We here concentrate on the case where $m_2 \geq 125$ GeV; in this case, $\sin\alpha \rightarrow 0$ corresponds to the SM decoupling. In figure 1, we show novel results for this model using currently available constraints^a, including a comparison of the currently maximal available rate of $H \rightarrow h_{125}h_{125}$ with the current combination limits from ATLAS²⁹. These plots supersede the results shown in^{27,30,28}. The most constraining direct search bound depends on the mass considered; in general, searches for diboson final states^{31,32,33,34} are most important, although some regions are also constrained from the Run 1 Higgs combination³⁵. Especially^{33,34} currently correspond to the best probes of the models parameter space^b.

4 Inert Doublet Model: sensitivity study

The Inert Doublet Model is a two Higgs doublet model (2HDM) that obeys an exact \mathbb{Z}_2 symmetry, leading to a dark matter candidate from the second scalar doublet^{36,37,38}. The results discussed here build on previous work^{39,26,27,40,41,42,43}. The model features four additional scalar states H, A, H^\pm , and has in total 7 free parameters prior to electroweak symmetry breaking

$$v, m_h, \underbrace{m_H, m_A, m_{H^\pm}}_{\text{second doublet}}, \lambda_2, \lambda_{345} \equiv \lambda_3 + \lambda_4 + \lambda_5, \quad (2)$$

where the λ_i s are standard couplings appearing in the 2HDM potential. Two parameters (m_h and v) are fixed by current measurements.

The discovery potential for ILC/ CLIC has been discussed in^{41,42,44}, including detailed signal and background simulation, beam-strahlung, etc. We here focus on the results of⁴³, where a

^aCollider constraints are implemented via the current versions of HiggsBounds/ HiggsSignals.

^bWe include searches currently available via HiggsBounds.

collider	all others	AA	AA +VBF
HL-LHC	1 TeV	200-600 GeV	500-600 GeV
HE-LHC	2 TeV	400-1400 GeV	800-1400 GeV
FCC-hh	2 TeV	600-2000 GeV	1600-2000 GeV
CLIC, 3 TeV	2 TeV	-	300-600 GeV
$\mu\mu$, 10 TeV	2 TeV	-	400-1400 GeV
$\mu\mu$, 30 TeV	2 TeV	-	1800-2000 GeV

Table 1: Sensitivity of different collider options, using the sensitivity criterium of 1000 generated events in the specific channel. $x - y$ denotes minimal/ maximal mass scales that are reachable.

sensitivity comparison for selected benchmark points^{40,41,43} using a simple counting criteria was presented: a benchmark point is considered reachable if at least 1000 signal events are produced using nominal luminosity of the respective collider (c.f. also⁴⁵). The summary of sensitivities in terms of mass scales is given in table 1, and a graphical display in terms of production cross sections for pair-production of the novel scalars at various collider options and center-of-mass energies in figure 2, taken from⁴³. All cross-sections have been calculated using Madgraph5⁴⁶ with a UFO input file from^{47c}. Results for CLIC were taken from^{41,42}.

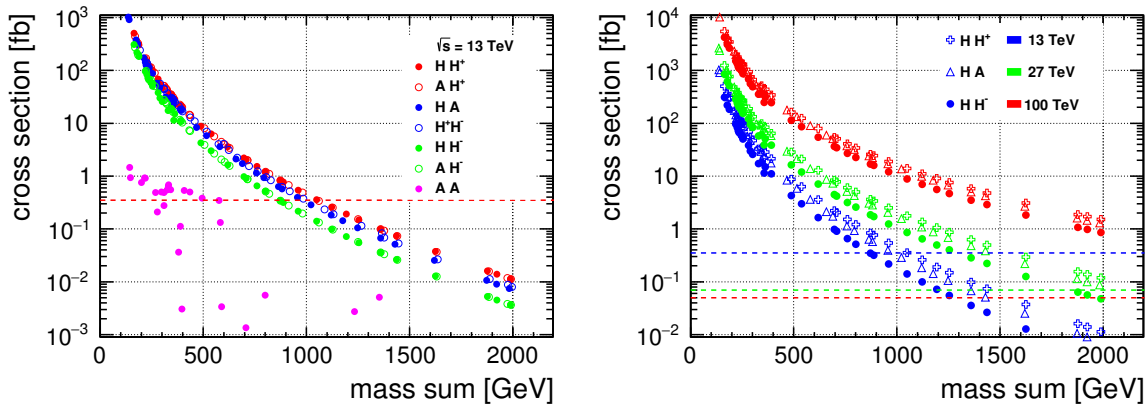


Figure 2 – Pair-production cross-section predictions at pp colliders as a function of the sum of produced particle masses. *Left*: For all considered production channels at 13 TeV LHC. *Right*: for selected channels at 13 TeV, 27 TeV, and 100 TeV. Horizontal dashed lines denote the limit of the cross section at which 1000 events are produced with the respective target luminosity.

We also include predictions in the VBF-type mode, corresponding to

$$pp \rightarrow X + jj, \mu^+ \mu^- \rightarrow X + \nu_\mu \bar{\nu}_\mu \quad (3)$$

for proton-proton collisions and processes at a muon collider, where X signifies the corresponding final state. The cross sections are displayed in figure 3, taken from⁴³. We see that especially for AA production the VBF mode serves to significantly increase the discovery reach of the respective machine. Using the simple counting criterium above, we can furthermore state that a 27 TeV proton-proton machine has a similar reach as a 10 TeV muon collider, while 100 TeV FCC-hh would correspond to a 30 TeV muon-muon machine.

^c Note the official version available at⁴⁸ exhibits a wrong CKM structure, leading to false results for processes involving electroweak gauge bosons radiated off quark lines. In our implementation in⁴³, we corrected for this. Our implementation corresponds to the expressions available from⁴⁹.

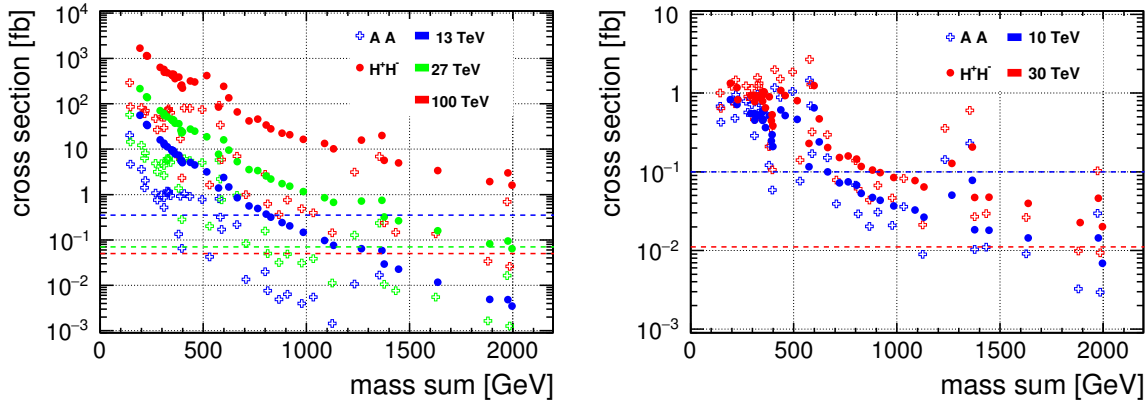


Figure 3 – As figure 2, but now considering the VBF-type production mode. *Left*: for pp colliders, where two additional jets are produced and *right*: at $\mu\mu$ colliders.

5 2 real singlet extension: triple-Higgs final states

We now discuss the model introduced in ⁵⁰, where the scalar sector of the SM is extended by two real scalars with a discrete $\mathbb{Z}_2 \otimes \mathbb{Z}'_2$ symmetry, that is explicitly broken by the vevs of the two scalar fields, leading to mixing between all scalar states. The model is characterized by 9 parameters after electroweak symmetry breaking

$$m_1, m_2, m_3, v, v_X, v_S, \theta_{hS}, \theta_{hX}, \theta_{SX}, \quad (4)$$

where m_i, v, θ denote masses^d, vevs, and mixing angles. As before, one mass m and v are fixed.

In ⁵⁰, various benchmark planes were proposed within this model, allowing for processes which by that time had not been investigated by the LHC experiments:

$$pp \rightarrow h_3 \rightarrow h_1 h_2, pp \rightarrow h_a \rightarrow h_b h_b \quad (5)$$

where in the latter case $h_a, h_b \neq h_{125}$ such that none of the scalars is identified with the 125 GeV resonance. We here focus on BP3, which features the first production mode, in the scenario with $h_1 \equiv h_{125}$. Depending on m_2 , this allows for a $h_{125} h_{125} h_{125}$ final state. For the subsequent decay $h_{125} \rightarrow b\bar{b}$, this point was investigated in ⁵¹ at a 14 TeV LHC, including detailed signal and background simulation, where we made use of a customized `loop_sm` model implemented in `MadGraph5_aMC@NLO` (v2.7.3)^{52,53}, and subsequently interfaced to `HERWIG` (v7.2.1)^{54,55,56,57,58,59,60}. Results are shown in table 2. We see that using the analysis strategy of⁵¹, several benchmark points are already accessible with a relatively low integrated luminosity.

6 Conclusion

A detailed understanding of the scalar sector realized by Nature is one of the most important tasks at current and future collider facilities. We have presented results for several models that extend the scalar sector of the SM by additional scalar states, and reported on the current status as well as future collider prospects.

Acknowledgments

The author thanks all her collaborators who made the achievements of the results discussed here possible. This research was supported in parts by the National Science Centre, Poland,

^dWe use the convention $m_1 \leq m_2 \leq m_3$.

(m_2, m_3) [GeV]	$\sigma(pp \rightarrow h_1 h_1 h_1)$ [fb]	$\sigma(pp \rightarrow 3b\bar{b})$ [fb]	$\text{sig} _{300\text{fb}^{-1}}$	$\text{sig} _{3000\text{fb}^{-1}}$
(255, 504)	32.40	6.40	2.92	9.23
(263, 455)	50.36	9.95	4.78	15.10
(287, 502)	39.61	7.82	4.01	12.68
(290, 454)	49.00	9.68	5.02	15.86
(320, 503)	35.88	7.09	3.76	11.88
(264, 504)	37.67	7.44	3.56	11.27
(280, 455)	51.00	10.07	5.18	16.39
(300, 475)	43.92	8.68	4.64	14.68
(310, 500)	37.90	7.49	4.09	12.94
(280, 500)	40.26	7.95	4.00	12.65

Table 2: 6 b final state leading-order production cross sections at 14 TeV, as well as significances for different integrated luminosities.

the HARMONIA project under contract UMO-2015/18/M/ST2/00518 and OPUS project under contract UMO-2017/25/B/ST2/00496 (2018-2021), by the European Union through the Programme Horizon 2020 via the COST actions CA15108 - FUNDAMENTALCONNECTIONS and CA16201 - PARTICLEFACE, and by the UK's Royal Society.

References

1. D. Eriksson, J. Rathsman, and O. Stal, *Comput. Phys. Commun.* **181**, 189 (2010), 0902.0851.
2. D. Eriksson, J. Rathsman, and O. Stal, *Comput. Phys. Commun.* **181**, 833 (2010).
3. R. Coimbra, M. O. P. Sampaio, and R. Santos, *Eur. Phys. J.* **C73**, 2428 (2013), 1301.2599.
4. M. Muehlleitner, M. O. P. Sampaio, R. Santos, and J. Wittbrodt, (2020), 2007.02985.
5. P. Bechtle, O. Brein, S. Heinemeyer, G. Weiglein, and K. E. Williams, *Comput. Phys. Commun.* **181**, 138 (2010), 0811.4169.
6. P. Bechtle, O. Brein, S. Heinemeyer, G. Weiglein, and K. E. Williams, *Comput. Phys. Commun.* **182**, 2605 (2011), 1102.1898.
7. P. Bechtle *et al.*, *PoS CHARGED2012*, 024 (2012), 1301.2345.
8. P. Bechtle *et al.*, *Eur. Phys. J.* **C74**, 2693 (2014), 1311.0055.
9. P. Bechtle, S. Heinemeyer, O. Stal, T. Stefaniak, and G. Weiglein, *Eur. Phys. J.* **C75**, 421 (2015), 1507.06706.
10. <https://higgsbounds.hepforge.org/>.
11. P. Bechtle *et al.*, *Eur. Phys. J.* **C80**, 1211 (2020), 2006.06007.
12. O. Stål and T. Stefaniak, *PoS EPS-HEP2013*, 314 (2013), 1310.4039.
13. P. Bechtle, S. Heinemeyer, O. Stal, T. Stefaniak, and G. Weiglein, *Eur. Phys. J.* **C74**, 2711 (2014), 1305.1933.
14. P. Bechtle, S. Heinemeyer, O. Stal, T. Stefaniak, and G. Weiglein, *JHEP* **11**, 039 (2014), 1403.1582.
15. P. Bechtle *et al.*, *Eur. Phys. J.* **C81**, 145 (2021), 2012.09197.
16. G. Belanger, F. Boudjema, A. Goudelis, A. Pukhov, and B. Zaldivar, *Comput. Phys. Commun.* **231**, 173 (2018), 1801.03509.
17. G. Belanger, A. Mjallal, and A. Pukhov, *Eur. Phys. J.* **C81**, 239 (2021), 2003.08621.
18. Gfitter Group, M. Baak *et al.*, *Eur. Phys. J.* **C74**, 3046 (2014), 1407.3792.
19. <http://project-gfitter.web.cern.ch/project-gfitter/>.
20. J. Haller *et al.*, *Eur. Phys. J.* **C78**, 675 (2018), 1803.01853.
21. Planck, N. Aghanim *et al.*, *Astron. Astrophys.* **641**, A6 (2020), 1807.06209.
22. XENON, E. Aprile *et al.*, *Phys. Rev. Lett.* **121**, 111302 (2018), 1805.12562.

23. G. M. Pruna and T. Robens, *Phys. Rev.* **D88**, 115012 (2013), 1303.1150.
24. T. Robens and T. Stefaniak, *Eur. Phys. J.* **C75**, 104 (2015), 1501.02234.
25. T. Robens and T. Stefaniak, *Eur. Phys. J.* **C76**, 268 (2016), 1601.07880.
26. LHC Higgs Cross Section Working Group, D. de Florian *et al.*, (2016), 1610.07922.
27. A. Ilnicka, T. Robens, and T. Stefaniak, *Mod. Phys. Lett.* **A33**, 1830007 (2018), 1803.03594.
28. J. Alison *et al.*, (2019), 1910.00012, [Rev. Phys.5,100045(2020)].
29. ATLAS, G. Aad *et al.*, *Phys. Lett.* **B800**, 135103 (2020), 1906.02025.
30. T. Robens, *PoS LHCP2019*, 138 (2019), 1908.10809.
31. CERN Report No., , 2013 (unpublished), CMS-PAS-HIG-13-003.
32. CMS, V. Khachatryan *et al.*, *JHEP* **10**, 144 (2015), 1504.00936.
33. CMS, A. M. Sirunyan *et al.*, *JHEP* **06**, 127 (2018), 1804.01939, [Erratum: *JHEP*03,128(2019)].
34. ATLAS, M. Aaboud *et al.*, *Phys. Rev.* **D98**, 052008 (2018), 1808.02380.
35. CERN Report No., , 2012 (unpublished), CMS-PAS-HIG-12-045.
36. N. G. Deshpande and E. Ma, *Phys. Rev.* **D18**, 2574 (1978).
37. Q.-H. Cao, E. Ma, and G. Rajasekaran, *Phys. Rev.* **D76**, 095011 (2007), 0708.2939.
38. R. Barbieri, L. J. Hall, and V. S. Rychkov, *Phys. Rev.* **D74**, 015007 (2006), hep-ph/0603188.
39. A. Ilnicka, M. Krawczyk, and T. Robens, *Phys. Rev.* **D93**, 055026 (2016), 1508.01671.
40. J. Kalinowski, W. Kotlarski, T. Robens, D. Sokolowska, and A. F. Zarnecki, *JHEP* **12**, 081 (2018), 1809.07712.
41. J. Kalinowski, W. Kotlarski, T. Robens, D. Sokolowska, and A. F. Zarnecki, *JHEP* **07**, 053 (2019), 1811.06952.
42. R. Franceschini *et al.*, (2018), 1812.02093.
43. J. Kalinowski, T. Robens, D. Sokolowska, and A. F. Zarnecki, (2020), 2012.14818.
44. A. F. Zarnecki *et al.*, Searching Inert Scalars at Future e^+e^- Colliders, in *International Workshop on Future Linear Colliders (LCWS 2019) Sendai, Miyagi, Japan, October 28-November 1, 2019*, 2020, 2002.11716.
45. T. Robens, J. Kalinowski, A. F. Zarnecki, and A. Papaefstathiou, Extended scalar sectors at future colliders, 2021, 2104.00046.
46. J. Alwall, M. Herquet, F. Maltoni, O. Mattelaer, and T. Stelzer, *JHEP* **06**, 128 (2011), 1106.0522.
47. A. Goudelis, B. Herrmann, and O. Stål, *JHEP* **09**, 106 (2013), 1303.3010.
48. <https://feynrules.irmp.ucl.ac.be/wiki/ModelDatabaseMainPage>, (as checked on Dec. 18,2020).
49. Particle Data Group, P. A. Zyla *et al.*, *PTEP* **2020**, 083C01 (2020).
50. T. Robens, T. Stefaniak, and J. Wittbrodt, *Eur. Phys. J.* **C80**, 151 (2020), 1908.08554.
51. A. Papaefstathiou, T. Robens, and G. Tetlalmatzi-Xolocotzi, (2020), 2101.00037.
52. J. Alwall *et al.*, *JHEP* **07**, 079 (2014), 1405.0301.
53. V. Hirschi and O. Mattelaer, *JHEP* **10**, 146 (2015), 1507.00020.
54. M. Bahr *et al.*, *Eur. Phys. J.* **C58**, 639 (2008), 0803.0883.
55. S. Gieseke *et al.*, (2011), 1102.1672.
56. K. Arnold *et al.*, (2012), 1205.4902.
57. J. Bellm *et al.*, (2013), 1310.6877.
58. J. Bellm *et al.*, *Eur. Phys. J.* **C76**, 196 (2016), 1512.01178.
59. J. Bellm *et al.*, (2017), 1705.06919.
60. J. Bellm *et al.*, *Eur. Phys. J.* **C80**, 452 (2020), 1912.06509.